

# Eddy diffusivity in homogeneous isotropic turbulence

Yasaman Shirian\* and Ali Mani†

Center for Turbulence Research, Stanford University, Stanford, California 94305, USA

In this study, we use the macroscopic forcing method to compute the scale-dependent eddy diffusivity for mean scalar and momentum transport by incompressible homogeneous isotropic turbulence. While for scales larger than the large eddy length, a Boussinesq-type behavior is observed, eddy diffusivity is found to vanish inversely proportional to the wavenumber for small scales. Behavior at all scales is found to be reasonably captured by a non-local eddy diffusivity operator modeled as  $D/\sqrt{1 - l^2 \nabla^2}$ , where  $D$  is the eddy diffusivity in the Boussinesq limit, and  $l$  is a constant on the order of the large-eddy length. Additionally, by comparing transport of momentum to that of passive scalars we present a quantification of the scale-dependent turbulent Schmidt number. Our results suggest that turbulent fluxes in response to mean momentum gradients are more local than fluxes in response to mean scalar gradients. These results have major implications in turbulence modeling in the context of the Reynolds-averaged Navier-Stokes equation and large-eddy simulations.

## INTRODUCTION

Over the past decades, experimental rheometry has been used as a tool for quantitative characterization of momentum transport by fluids [1]. For incompressible Newtonian fluids, the momentum diffusion rate is proportional to the strain-rate tensor. However, the proportionality constant, called molecular diffusivity or viscosity, needs to be quantified for each fluid. Rheometers, measure momentum diffusivity by subjecting a given fluid to a measurable strain rate, where it sustains momentum diffusion that is measurable in terms of an applied force. Such measurements are critical to the closure of transport models allowing scale-up of molecular dynamic processes to continuum-level equations such as the Navier-Stokes equation.

Aligned with this mindset, scaled-up models have been pursued for turbulent flows [2],[3]. In such models, mathematical closures critically rely on a description of averaged momentum diffusion due to the underlying turbulent fluctuations. This is where experimental rheometry faces challenges, since one of the working principles of rheometry is that it must be non-intrusive to the mechanism of momentum transport while manipulating momentum itself. For laminar flows, this principle means rheometry must not affect the underlying molecular dynamic processes. For turbulent flows, however, to be non-intrusive to the mechanism of momentum transport, rheometers must not change the turbulent eddies of such flows while straining them!

In a recent work, we developed a computational method, called the macroscopic forcing method (MFM), that overcomes this shortcoming [4]. In this methodology one can computationally simulate a turbulent flow, and “measure” its mean momentum diffusivity, like a rheometer, in a manner non-intrusive to the mechanism of momentum transport. This is achieved by solving a

generalized momentum transport equation (GMT):

$$\frac{\partial v_i}{\partial t} + \frac{\partial}{\partial x_j} (u_j v_i) = -\frac{1}{\rho} \frac{\partial q}{\partial x_i} + \nu \frac{\partial^2 v_i}{\partial x_j \partial x_j} + s_i, \quad (1)$$

where  $v_i$  represents momentum per unit mass,  $\rho$  and  $\nu$  are fluid density and molecular diffusivity, and  $q$  is the pressure required to satisfy the constraint  $\partial v_i / \partial x_i = 0$ .  $u_j$  is the given turbulent flow whose “eddy diffusivity” is to be measured. Here eddy diffusivity characterizes the rate of mean momentum flux by turbulent eddies in response to mean momentum gradients. For a given turbulence condition,  $u_j$  can be obtained from a separate direct numerical simulation or from experimental measurements.  $s_i$  is the macroscopic forcing that acts similar to the way that a rheometer forces a fluid. However, here the forcing is not limited to the boundaries, allowing one to probe non-localities in eddy diffusivity.

Equation (1) is a generalization of the Navier-Stokes equation in the sense that it does not constrain  $\mathbf{u}$  to be equal to  $\mathbf{v}$ , by recognizing the fact that the former represents a kinematic transporter of momentum and the latter represents momentum itself. With this decoupling, one can perform rheometry by maintaining the principle of being non-intrusive to the mechanism of momentum transport,  $\mathbf{u}$ , while manipulating the momentum field,  $\mathbf{v}$ .

This study reports the first application of MFM for measurement of eddy diffusivity in a turbulent flow. As a model problem, we consider homogeneous isotropic turbulence and present not only its scale-dependent eddy diffusivity, but also reveal the quantitative differences in eddy-diffusivity between transport of scalar and momentum fields.

## COMPUTATIONAL METHODS

We performed direct numerical simulation (DNS) of incompressible homogeneous and isotropic turbulence in

a triply periodic cubic domain of size  $2\pi \times 2\pi \times 2\pi$  using uniform structured meshes. To sustain turbulence in a time-stationary fashion, we solved the Navier-Stokes equation subject to a forcing described by

$$\frac{\partial u_i}{\partial t} + \frac{\partial}{\partial x_j} (u_j u_i) = -\frac{1}{\rho} \frac{\partial p}{\partial x_i} + \nu \frac{\partial^2 u_i}{\partial x_j \partial x_j} + A u_i, \quad (2)$$

where  $A$  is the forcing constant. Table I represents the nominal Reynolds numbers,  $\text{Re}_\lambda$  for each simulation, and the specified  $A$  and  $\nu$  following the prescription of [5]. Additionally, the table lists the single component velocity fluctuations  $u_{\text{rms}}$ , turbulent dissipation rate  $\varepsilon = -\nu \overline{u_i \nabla^2 u_i}$ , where the overline indicates statistical averaging, and the eddy size defined as  $l_{\text{eddy}} = u_{\text{rms}}^3 / \varepsilon$ . These statistics are obtained from post-processing the DNS data, with the error intervals indicating the statistical error of the means due to finite sampling. The simulation times, reported in the table in units of  $t_{\text{eddy}} = l_{\text{eddy}} / u_{\text{rms}}$ , are sufficiently long to allow reporting of the statistics with the given number of significant digits.

For these simulations, we adopted the code of [6] under the incompressible mode. The same code was used for numerical solutions to Equation (1) after slight modification to allow  $u_j$  and  $v_i$  to be different vector fields and adjusting the forcing functions. Additionally, for each flow field  $u_j$ , we solved the forced passive scalar equation,

$$\frac{\partial c}{\partial t} + \frac{\partial}{\partial x_j} (u_j c) = \nu \frac{\partial^2 c}{\partial x_j \partial x_j} + s, \quad (3)$$

in order to analyze eddy diffusivity of scalar fields with the same  $\nu$  as that in the momentum equation.

Below we describe the details of the analysis steps leading to the determination of eddy diffusivity for mean scalar transport. Similar steps are taken for determination of eddy diffusivity for mean momentum transport.

Ensemble averaging of Equation (3) leads to the transport equation governing the mean fields,

$$\overline{\mathcal{L}'_c \bar{c}} = \nu \nabla^2 \bar{c} + s, \quad (4)$$

where  $\overline{\mathcal{L}'_c}$  is the macroscopic closure operator that can be expressed as  $\overline{\mathcal{L}'_c} = -\nabla \cdot \mathcal{D}_c \nabla$ , where  $\mathcal{D}_c$  is the eddy diffusivity operator. We use the subscript  $c$  to denote operators associated with mean scalar transport. Later, the subscript  $v$  is used to denote operators associated with mean momentum transport.

By selecting harmonic forcing functions of the form  $s = \exp(i\mathbf{k}\mathbf{x})$ , and utilizing DNS of (3), we obtain a harmonic mean response of the form  $\bar{c} = \widehat{\bar{c}}(\mathbf{k}) \exp(i\mathbf{k}\mathbf{x})$  as shown in Figure 1. Substitution in (4) leads to determination of the macroscopic closure operator in Fourier space as  $\widehat{\mathcal{L}'_c}(\mathbf{k}) = 1/\widehat{\bar{c}} - |\mathbf{k}|^2 \nu$ , and the eddy diffusivity operator as  $\widehat{\mathcal{D}_c}(\mathbf{k}) = \widehat{\mathcal{L}'_c} / |\mathbf{k}|^2$ . Given the isotropy of the underlying flow,  $\widehat{\mathcal{L}'_c}$  and  $\widehat{\mathcal{D}_c}$  are functions of  $k = |\mathbf{k}|$ , and therefore it is sufficient to consider wavenumbers only in the  $x_1$

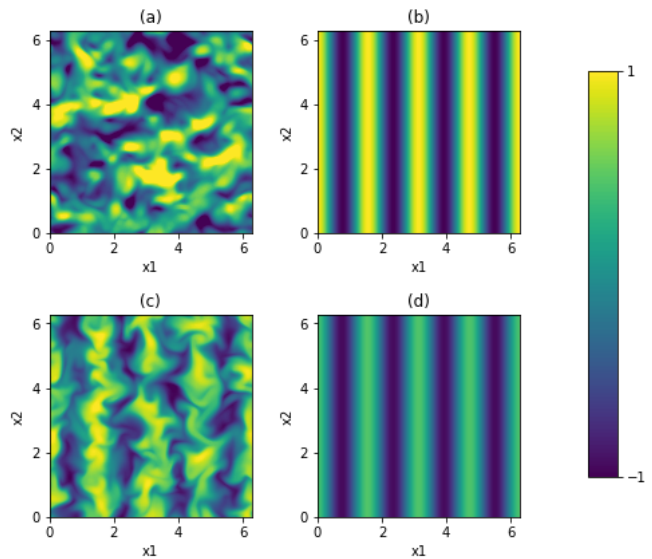


FIG. 1. (a) A snapshot of the HIT simulation representing a component of the velocity field (b) The real part of macroscopic force,  $s$ , for mode  $k = 4$  (c) A 2D snapshot of the instantaneous scalar field,  $c$ , subject to the given flow and  $s$  (d) The mean scalar field  $\bar{c}$ .

direction. For each forcing scenario,  $s(k, x_1)$ , we perform DNS of Equation (3), and obtain  $\bar{c}(k, x_1)$  by averaging the solution in time as well as  $x_2$  and  $x_3$  directions.  $\bar{c}(k)$  is computed by evaluating the  $k^{\text{th}}$  Fourier mode of  $\bar{c}$ , and verifying that the other modes are statistically zero, as visually seen in Figure 1d. A similar approach is used for determination of  $\overline{\mathcal{L}'_v}$  and  $\mathcal{D}_v$  by solving (1) in response to forcing of the form  $s_2 = \exp(ikx_1)$ ,  $s_1 = s_3 = 0$ .

For each flow Reynolds number, equations (1) and (3) are solved for  $k=0.25, 0.5, 1, 2, 4$ , and  $8$ . For cases with  $k < 1$  equations (1) and (3) are solved in domains with length  $8\pi$  in the  $x_1$  direction where the velocity field  $u_j$  is obtained by four times copying the nominal periodic HIT solution.

The computational grids use  $64^3$ ,  $128^3$ , and  $256^3$  mesh points respectively for cases with  $\text{Re}_\lambda = 26, 40$  and  $67$ . The only exception is the case of  $\text{Re}_\lambda = 26$  and  $k=8$  where a  $128^3$  mesh is used to allow more accuracy in capturing high wavenumbers.

In addition to these calculations, we analyzed cases to study the limit of  $k = 0$ . In this limit, one can assume locally linear mean profiles as  $\bar{c} = x_1$  while fluctuations remain statistically locally homogeneous. In other words, MFM analysis of scalar transport in the limit of  $k \rightarrow 0$  collapses to methods described in homogenization theories [7]. According to these methods, one can substitute the linear mean explicitly in the governing equations, e.g., Equation (3), and obtain a direct equation for fluctuating quantities that can be solved on a periodic domain. In this case we used the inverse macroscopic forcing methodology (IMFM)[4] to compute the eddy-

TABLE I. Simulation parameters and flow statistics, reported uncertainties are statistical error of the mean

$Re_\lambda$	$A$	$\nu$	$u_{\text{rms}}$	$\varepsilon$	$l_{\text{eddy}}$	$T_{\text{final}}/t_{\text{eddy}}$
26	0.2792	0.0263	$0.97 \pm 0.002$	$0.790 \pm 0.004$	$1.15 \pm 0.02$	$O(1500)$
40	0.2792	0.0111	$0.90 \pm 0.002$	$0.679 \pm 0.004$	$1.07 \pm 0.02$	$O(500)$ - $O(1000)$
67	0.2792	0.0039	$1.00 \pm 0.03$	$0.84 \pm 0.05$	$1.20 \pm 0.03$	$O(200)$

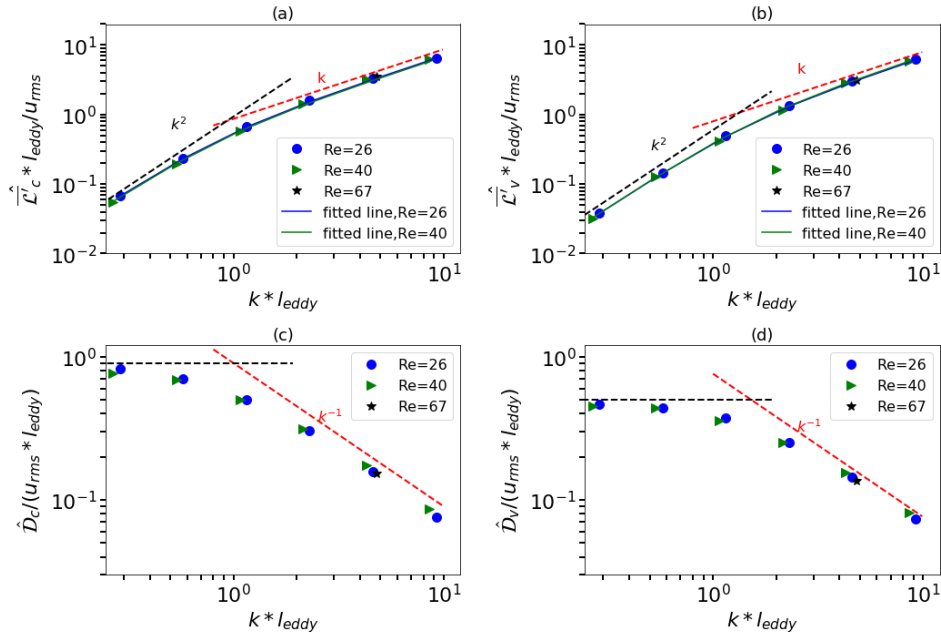


FIG. 2. Measured macroscopic closure operators versus wavenumber for transport of (a) scalars and (b) momentum as well as the corresponding eddy diffusivity operators as shown in (c) and (d).

diffusivity coefficient. We extended the same method for analysis of Equation (1) in the limit of  $k \rightarrow 0$ .

## RESULTS

Figure 2 shows the computed macroscopic closure operators as well as the corresponding eddy diffusivity operators for both scalar and momentum transport over a range of wavenumbers and Reynolds numbers. Scaling of data in units of  $u_{\text{rms}}$  and  $l_{\text{eddy}}$  results in reasonable collapse of data suggesting weak sensitivity on the Reynolds number. The slight decrease of both  $l$  and  $D$  with the Reynolds number can be explained by the fact that at higher  $Re_\lambda$  a slightly larger portion of  $u_{\text{rms}}$  occurs at small scale, which is less effective in macroscopic mixing. However, given that in the limit of  $Re \rightarrow \infty$  a finite portion of energy exists at small scales, We anticipate a diminishing sensitivity of  $l$  and  $D$  on  $Re_\lambda$  in that limit.

All results in the limit of small  $k$  indicate  $\hat{\mathcal{L}} \sim k^2$ , and a constant eddy diffusivity  $\hat{D} \sim k^0$  consistent with the Boussinesq approximation [8].

In the large wavenumber limit, however, the true closure operator significantly departs from that of Boussi-

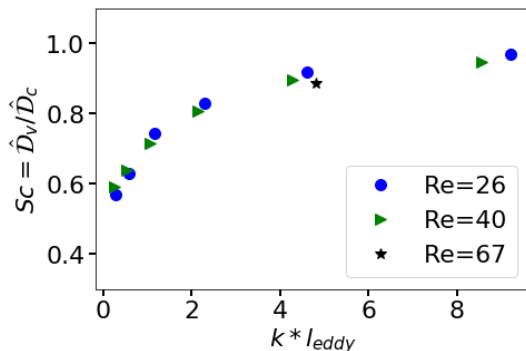


FIG. 3. Schmidt number versus dimensionless wavenumber

nesq limit. In this case, the eddy diffusivity drops inversely proportional to the wavenumber. This departure can be explained intuitively as follows. Standard diffusion implies that transported quantities propagate in space proportional to square root of time,  $x \sim \sqrt{t}$ , resulting in unbounded characteristic speed over short distance. However, given that here the underlying mechanism of transport is advection, transported quantities cannot propagate faster than linearly with time. In fact,

TABLE II. Coefficients in the fitted curve  $Dk^2/\sqrt{1+(lk)^2}$  for macroscopic closure operator  $\widehat{\mathcal{L}}'(k)$ .  $D$  is reported in units of  $u_{\text{rms}}l_{\text{eddy}}$ , and  $l$  is reported in units of  $l_{\text{eddy}}$

	$D_c$	$D_v$	$l_c$	$l_v$
$Re_\lambda = 26$	0.86	0.46	1.23	0.69
$Re_\lambda = 40$	0.83	0.46	1.13	0.67

$k^1$  is an upper bound for a power law scaling of  $\widehat{\mathcal{L}}'$  in the large  $k$  limit.  $\widehat{\mathcal{L}}'$  obtained from this study simply satisfies this physical limitation.

Another interesting observation is that although the scaling of the macroscopic closure operator in the limit of large  $k$  is advective,  $\widehat{\mathcal{L}}' \sim u_{\text{rms}}k$ , the closure operator itself is not an advection operator. Instead, it is a dissipative operator but with advective scaling, since the prefactor to the scaling is real and positive, and not imaginary. This result, translated to physical space, implies that  $\widehat{\mathcal{L}}' \sim u_{\text{rms}}\sqrt{\nabla^2}$ , in the high-wavenumber limit where  $\nabla^2$  is the Laplacian operator.

Matching the two asymptotic limits of small and large  $k$ , we identify the following expression as a uniformly valid approximation for the macroscopic closure operator

$$\widehat{\mathcal{L}}' = \frac{Dk^2}{\sqrt{1+l^2k^2}}, \quad (5)$$

where the constants  $D$  and  $l$  are reported in Table II and fitted to match the computed  $\widehat{\mathcal{L}}'$  for  $k \rightarrow 0$  and  $k = 8$ . As shown in Figure 2a and b, this expression matches the numerically computed  $\widehat{\mathcal{L}}'$  over all ranges of  $k$ . This operator expressed in physical space is  $\widehat{\mathcal{L}}' = \nabla \cdot \mathcal{D} \nabla$ , where the eddy diffusivity operator,  $\mathcal{D}$  can be expressed as

$$\mathcal{D} = \frac{D}{\sqrt{\mathcal{I} - l^2 \nabla^2}}, \quad (6)$$

where  $\mathcal{I}$  represents the identity operator. The denominator in (6) is an inverse operator, which indicates the non-locality of eddy diffusivity.  $l$ , which is on the order of the large eddy size, quantifies the extent of the non-locality, i.e, a measure of how far the mean gradients at one location can influence mean fluxes at another location. This constant, plays a role similar to the mean free path in molecular systems.

The fact that  $l_v$  is smaller than  $l_c$  (see Table II) indicates that the macroscopic closure operator is more local for momentum transport than for scalar transport. This is an unintuitive result, since at the DNS level, scalar transport is completely local, while momentum transport involves a non-local pressure projection. We conclude that at the macroscopic level, the non-locality of pressure cancels a portion of non-locality of advection.

Lastly, we show in Figure 3 the scale-dependent turbulent Schmidt number defined as  $Sc(k) = \widehat{\mathcal{D}}_v/\widehat{\mathcal{D}}_c$ . Unlike prior estimates, where the turbulent Schmidt number is inferred from DNS by assuming a local eddy diffusivity as the model-form [9],[10], here we provide a direct quantification without constraining the model form. While  $Sc$  is an  $O(1)$  quantity, we observe that it monotonically varies from about 0.5 in the low wavenumber limit to about 1 in the high wavenumber limit.

## DISCUSSIONS

The work presented here has crucial implications in turbulence modeling. In this context, a long-standing challenge has been the determination and validation of model forms for turbulence closures. The results presented here provide the first quantification of a turbulence model form by considering a canonical setting. As a measure of its practical utility, we show in [4] that the same model form introduced in Equation (6) offers significant improvements in RANS (Reynolds-Averaged Navier-Stokes) prediction of axisymmetric turbulent jet flow. We anticipate the same model form will improve explicitly filtered large-eddy simulations, given the universality of the limitation of standard eddy diffusivity in providing bounded characteristic speeds over short distances. In this case,  $D$  and  $l$  must be scaled in units of subgrid scale kinetic energy and the filter size assuming the subgrid scale flow is analogous to the turbulent box flows analyzed here. Extension of the presented methodology to more complex flows allows the discovery of appropriate anisotropic and inhomogeneous turbulence model forms. Such extensions will also provide a systematic framework for assessment of existing models by allowing independent quantification of errors in model coefficients versus model forms, thus eliminating possible ambiguities due to error cancellation between the two.

## ACKNOWLEDGEMENTS

The study presented in this report was supported by the Boeing company under grant number SPO 134136 and the U.S. Department of Energy, under grant number de-na0002373.

\* yshirian@stanford.edu

† alimani@stanford.edu

- [1] W. C. Macosko, *Rheology: Principles, Measurements, and Applications* (Wiley-VCH, 1994).
- [2] C. G. Speziale, Annual Review of Fluid Dynamics **23**, 107 (1991).

- [3] P. A. Durbin, Annual Review of Fluid Dynamics **50**, 77 (2018).
- [4] A. Mani and D. Park, Physical Review Fluids (under review).
- [5] C. Rosales and C. Meneveau, Physics of Fluids **17**, 095106 (2005).
- [6] H. Pouransari, M. Mortazavi, and A. Mani, arXiv preprint arXiv:1601.05448 (2016), <https://hadip@bitbucket.org/hadip/soleilmpi>.
- [7] A. Majda and P. R. kramer, Elsevier **314**, 1999 (1998).
- [8] J. Boussinesq, in *Mémoire présentés par divers savants à l'Académie des Sciences* **50**, 77 (Impr. nationale 1877).
- [9] P. Moin, K. Squires, W. Cabo, and S. Lee, Physics of Fluids **3**, 2746 (1991).
- [10] M. Rogers, P. Moin, and W. C. Reynolds, (1986), report No. TF-25, Stanford University, Mechanical Engineering Department.